

A Divide and Conquer Matrix Multiplication Algorithm to Speedup Algebraic Multigrid Setup

Anonymous
Anon University
Anonymous, Anonymous
anon@ymo.us

ABSTRACT

Algebraic Multigrid (AMG) is a popular solver and preconditioner for large sparse linear systems, especially the ones obtained from the discretization of elliptic operators. A key bottleneck for the scalability of the setup phase of AMG is the Matrix-matrix multiplication (MatMult) required for computing the sparse grid representation. While significant work has been done on optimizing matrix-matrix multiplication, in this work, we optimize it in the context of the matrix multiplications encountered in the setup phase of AMG. Specifically, we designed a new divide and conquer sparse MatMult, that is scalable and makes use of the specific structure of the restriction and prolongation matrices. This combined with an efficient communication pattern during parallel MatMult provides excellent performance for our AMG setup. We compare our solver with PETSc to demonstrate the performance improvements gained using our methods.

KEYWORDS

algebraic multigrid, AMG, sparse, matrix-matrix product, parallel

ACM Reference Format:

Anonymous. 2019. A Divide and Conquer Matrix Multiplication Algorithm to Speedup Algebraic Multigrid Setup. In *Proceedings of International Conference on Supercomputing (ICS'19)*. ACM, New York, NY, USA, 7 pages. <https://doi.org/10.1145/nnnnnnnn.nnnnnnnn>

1 INTRODUCTION

The solution of elliptic partial differential equation (PDE) operators forms the foundation of the mathematical models of several engineering applications. In solid mechanics, the stiffness matrix derived from linear elasticity represents an elliptic operator that, when discretized with the finite element method (FEM) yields a symmetric positive definite system. In fluid mechanics, the viscous terms and the pressure components of the incompressible Navier-Stokes equations, when discretized, often lead to symmetric positive definite systems. For the solution of such large-scale systems that need to be solved in parallel, iterative solvers with $O(n)$ complexity and mesh-independent convergence are preferred. The most popular methods in this regard have been the multigrid

methods—both geometric and algebraic. The geometric multigrid (GMG) methods when applied to matrices generated from regular (often evenly-spaced) discretizations of elliptic operators [3, 4, 7, 10]. The mathematical predictability of the benefits of the GMG approach combined with the ability to exploit the regularity of the data structures (in terms of indexing, coarsening, etc.) has made GMG, especially in conjunction with preconditioned conjugate gradient (PCG) [2, 16], the solver of choice when solving engineering applications that require large-scale parallel solution approaches. The story is more mixed when one moves to unstructured discretizations and corresponding to algebraic multigrid (AMG), the communities alternative to GMG for such problems.

While AMG is very attractive due to its black-box nature [6, 18, 19], it does not scale as well as GMG [14]. This is primarily due to the loss of sparsity at coarser levels arising from the Galerkin approximation [17], leading to poor scalability, especially at the coarser levels. Additionally, while both geometric and algebraic variants require an initial **setup** phase, the cost of the setup is significantly higher for AMG, making it less attractive unless multiple solves are performed for the same operator. This is clearly unattractive for dynamic systems where the operator is changing rapidly, such as systems with h or p enrichment. In such cases, while the cost of an AMG solve might be lower than say that of CG, the overall cost i.e., setup + solve might be more than using asymptotically inferior solvers. In most cases, the scalability of setup phase is also poor and typically worse than that of the solve phase. This is limited the attractiveness of AMG for large systems. In this work, we develop an efficient sparse matrix multiplication (MATMULT) algorithm to improve the performance and scalability of AMG. As will be explained in the following section, a sparse MATMULT is the dominant part of the AMG setup. While several of our optimizations apply to sparse MATMULT in general, and can be more broadly applied, our strategies for reducing inter-process communication make use of the special structure of MATMULT encountered during AMG setup.

1.1 Background

We start with a brief description of our AMG framework. AMG has been a popular method for solving the large-scale and often sparse linear system one obtains from discretization of elliptic partial differential equations. The linear system can be written as

$$Ax = b \quad (1)$$

in which, $A \in R^{n \times n}$, x and $b \in R^n$. AMG consists of a setup and a solve phase. The first step of the setup phase is to aggregate the nodes of the equivalent graph (G) of the matrix A . Every row of the matrix A is considered as a node in the graph G and there is an edge between nodes i and j if entry (i, j) is nonzero in A . After

Permission to make digital or hard copies of all or part of this work for personal or classroom use is granted without fee provided that copies are not made or distributed for profit or commercial advantage and that copies bear this notice and the full citation on the first page. Copyrights for components of this work owned by others than ACM must be honored. Abstracting with credit is permitted. To copy otherwise, or republish, to post on servers or to redistribute to lists, requires prior specific permission and/or a fee. Request permissions from [permissions@acm.org](https://permissions.acm.org).
ICS'19, June 2019, Phoenix, Arizona, USA

aggregation, some nodes will be chosen as *roots* and the rest of the nodes of the graph will be assigned to them. Multiple aggregation methods for AMG have been introduced, such as [1], [12], [9], [11]. For this paper, *maximal independent set* from [1], with some modifications, is used.

Given a linear system we have n nodes in the graph G and m nodes are chosen as the *roots*. We compute prolongation P and Restriction R operators using the *roots*. The prolongation operator has two applications. It can interpolate a vector $v \in R^m$ to $v' \in R^n$, such that $m < n$. The other application is creating a coarse version of the operator A using the Galerkin approximation:

$$A_c = R \times A \times P \quad (2)$$

such that $A_c \in R^{m \times m}$. This operation is called *coarsening*. The restriction operator is used similarly. The triple MATMULT in (2) is the dominant cost of the AMG setup, especially when done in parallel. Improving the efficiency and scalability of this step in the main contribution of this work.

Progressively coarser versions of the matrix are created during the setup phase corresponding to a hierarchy (i.e. multi-level or "multigrid") of data structures. An AMG hierarchy of $L + 1$ levels consists of three categories of operators: coarse matrices (A_s), prolongation matrices (P_s) and restriction matrices (R_s).

The coarse matrices for each level are created similar to A_c :

$$A_s[l + 1] = R_s[l] \times A_s[l] \times P_s[l], \quad l = 0, 1, \dots, L$$

such that $A_s[0]$ is the finest matrix A . Again note that this is very expensive even at the coarser levels as the matrices get denser at the coarser levels. Our MATMULT maintains good performance and scalability across all levels of the multigrid hierarchy.

The next phase of AMG is the solve phase. To solve $Ax = b$, we start with an initial guess for x . The solution is computed in a recursive function *vcycle* (Algorithm 1). Regular smoothers are used in the relaxation part, such as Jacobi, Chebyshev, etc. Then, the residual r is computed. Next, r is taken to the coarser level by using the restriction operator (R). The function recurses until it reaches the coarsest level ($L + 1$). At that level, the system will be solved directly. The solution of that system is actually the error, which will be interpolated by P . After that, the solution will be corrected by subtracting the interpolated error from it. Finally, the solution will be smoothed again.

Algorithm 1 *vcycle*(g, x, b, l)

Input: *grid* g , b , x , and *level* (l)

Output: *solution* (x)

```

1: if  $l = L + 1$  then
2:    $x \leftarrow \text{direct solver}(g[L + 1], x, b)$ 
3: else
4:    $x \leftarrow \text{Smoother}(g, x, b, l)$ 
5:    $r \leftarrow A_s[l] \times x - b$ 
6:    $r_c \leftarrow R_s[l] \times r$ 
7:    $y_c \leftarrow \text{vcycle}(g, x, r_c, l + 1)$ 
8:    $y \leftarrow P_s[l] \times y_c$ 
9:    $x \leftarrow x - y$ 
10:   $x \leftarrow \text{Smoother}(g, x, b, l)$ 
11: end if
```

Smoothed Aggregation AMG (SA-AMG)[19] is a modified version of AMG, in which the prolongation and restriction operators are smoothed to improve the convergence of AMG. For this paper, the improved version of SA-AMG in [17] is used.

1.2 Related Work

While significant research has been done on improving the efficiency and scalability of sparse matrix-vector products, sparse MATMULT in comparison has received far less attention. Yuster and Zwick [20] provide a theoretically nearly optimal algorithm for multiplying sparse matrices, but rely on fast rectangular matrix multiplication. Consequently the approach is currently of only theoretical value. In [5], Buluc and Gilbert present algorithms for parallel sparse MATMULT using a two-dimensional block data distributions with serial hypersparse kernels. Gremse *et al.* [8] the authors present a promising algorithm using iterative row merging to improve the performance on GPUs. Similarly, Saule *et al.* [13] evaluate the performance of sparse matrix multiplication kernels on the Intel Xeon Phi. Most AMG implementation have relied on standard sparse MATMULT implementations without any special considerations for the structure of the matrices generated within AMG. This work attempts to fill this gap.

The main **contributions** of this work are,

- A new efficient MATMULT algorithm.
- A new method to communicate data required to do MATMULT specific to AMG

The rest of the paper is organized as follows. In §2 we discuss the different strategies used to improve the performance and scalability of MATMULT. In §3 we show the strong and weak scaling of our methods and compare our method with PETSc. Finally, we conclude the paper in §4.

2 METHODS

In this section, we present our matrix-matrix multiplication. We then explain further modifications to the triple matrix multiplication (2) that are part of the AMG setup process.

2.1 Matrix-Matrix Multiplication

We design a divide and conquer approach to perform the sparse MATMULT in a node-local fashion. The key idea is to perform simple tasks while recursing, having efficient memory access, and to perform the multiplication for small chunks where the resulting matrix can fit into an appropriate cache. For clarity of presentation, we assume that the data is available locally and discuss it as a serial implementation. Shared memory parallelism is added in a straightforward manner. We have implemented MATMULT in a recursive fashion. We split the matrices recursively in two ways: split by half based on the matrix size and based on number of nonzeros. First we explain the algorithms performing splitting based on the matrix sizes.

The recursive function, *RECURS_MATMULT*, includes three cases:

- (1) Case 1: Stop the recursion: perform the multiplication.
- (2) Case 2: A is horizontal.
- (3) Case 3: A is vertical.

2.1.1 Case 1. By splitting sparse matrices recursively, we will have more and more zero rows and columns in the resulting sub-matrices. So, using row size and column size of those sub-matrices is not very helpful. Instead, we use nonzero rows and nonzero columns. At the start of the recursive function, the number of nonzero rows of A (A_nnz_row) and nonzero columns of B (B_nnz_col) are being computed. A threshold for $NNZ_MAT_SIZE = A_nnz_row \times B_nnz_col$ is set. Our algorithm has a profiling step where it empirically determines the appropriate threshold by running several test cases. On the machines we used, $20M$ was chosen as the threshold. We continue splitting the matrices until the threshold is reached. Then, we preform the multiplication. We have implemented two methods for this case: dense data structure and hashmap.

When performing the multiplication, at least one of the matrices, typically the output, needs random access as it is accumulating the results. Given that the divide and conquer approach has reduced the size of the output matrix, the first approach is to keep a temporary buffer for dense matrix storage. Each nonzero of B is multiplied by its corresponding nonzero of A and the result will be added to the corresponding index in the dense matrix. As long as the dense matrix is small enough to fit within the L2 cache, we should get good performance. At the end of the multiplication, we traverse the dense matrix and extract the non-zeros as a sparse matrix. This approach works well as long as the resulting matrix is dense.

When NNZ_MAT_SIZE gets larger, it becomes inefficient to traverse the whole dense matrix and check for nonzeros in the final stage. To solve this issue, we use an efficient hashmap to achieve similar results without the $O(n^2)$ overhead of extracting the non-zeros from the dense matrix. The entry's index is the key and its value is the hashmap's value. When we want to add the multiplication of nonzeros of A and B to the hashmap, we check if the index exists in the map. If it exists the value is being added to the existing one's. Otherwise a new entry will be added to the hashmap. Clearly, there is an overhead to this approach that needs to be balanced against the overheads associated with the dense representation.

In Figure 1, we compare the two methods for computing coarse matrix $Ac = R \times A \times P$, in which A is the 3D Poisson problem of size $216k$. For $0 \leq NNZ_MAT_SIZE \leq 10M$, in $1M$ steps, we compare the two methods in order to develop an efficient hybrid algorithm. For instance, the first point indicates that the dense structure is better than hashmap in 1245 cases for all multiplications such that $0 \leq NNZ_MAT_SIZE < 1M$. For the lower range the dense representation is better and for the higher range the hashmap is significantly faster. Figure 2 shows the same experiment for matrix ID 1882 from SuiteSparse (Florida) Matrix Collection, which is a sparse matrix of size $1M$ and $5M$ nonzero.

A combination of these two methods would give us the best performance across different matrix structures and densities. The dense method is being used for the lower range and the hashmap for the higher range. We have done a series of experiments to determine the threshold when to switch between the two methods. Figures 1 and 2 suggest to use the dense structure method when $0 \leq NNZ_MAT_SIZE < 4M$ and use hashmap for the rest. We noticed that when hashmaps are better, the difference time between the two methods on average is higher. In other words, on average, n times performing hashmap is faster than n times using the dense

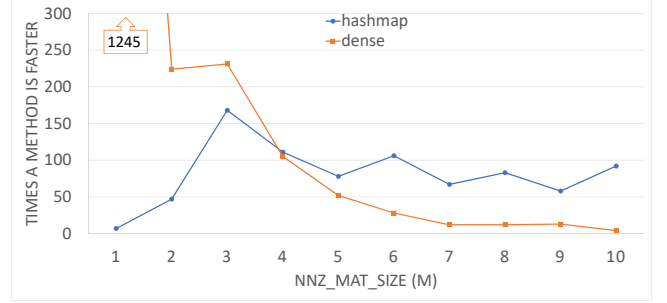


Figure 1: Comparison between dense structure method with hashmap to compute coarse matrix $Ac = R \times A \times P$, in which A is the 3D Poisson problem of size $216k$. The plot shows the number of times each method is faster than the other one in intervals of $1M$ for NNZ_MAT_SIZE .

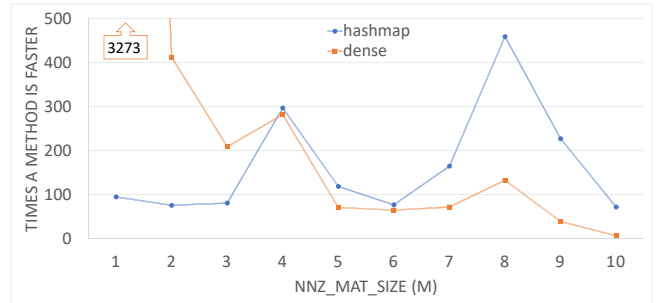


Figure 2: Comparison between dense structure method with hashmap to compute coarse matrix $Ac = R \times A \times P$, in which A is matrix ID 1882 from SuiteSparse (Florida) Matrix Collection. The plot shows the number of times each method is faster than the other one in intervals of $1M$ for NNZ_MAT_SIZE .

structure. So empirically, we found $1M$ to be a good estimate for switching between the two methods.

Figure 3 compares the hybrid method with the basic two methods. We have compared the the three approaches on different sizes of 3D Poisson problem, ranging from $8k$ to almost half a million. For instance, for the case where the matrix is of size $512k$, computing the first coarse matrix (performing the triple matrix) takes $291s$ if only hashmap is used for Case 1, takes $72s$ if only the dense structure is used and finally takes almost $17s$ when the hybrid approach is utilized for Case 1.

2.1.2 Case 2. When A is horizontal, i.e. its row size is less than or equal to its column size, we halve A by column based on its column size (Figure 4). Since row size of B equals column size of A , we halve B by row, so it will be a split similar to A , but horizontally. Then, the `RECURS_MATMULT` will be called twice, once on $A1$ and $B1$, and again on $A2$ and $B2$ (Algorithm 2). The results of the two multiplications will need to be added together at the end. It means, there will be entries for the result matrix with the same index, e.g. multiple entries with $(10, 20)$ as the index. We call these entries *duplicates*. Since there will be numerous nested recursive calls, we

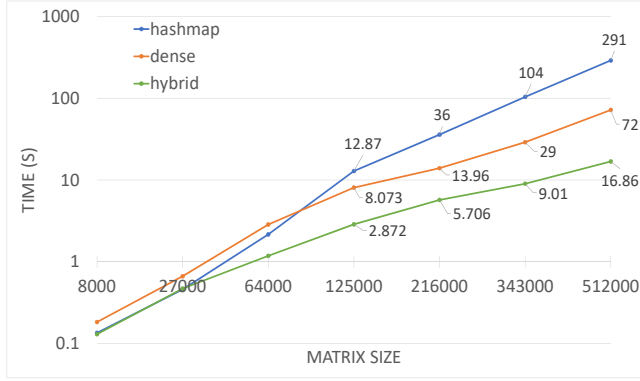


Figure 3: Comparison between the three methods to do Case 1: only using hashmap, only using the dense structure, and the hybrid method. They are used as Case 1 to compute the first coarse matrix (the triple multiplication) on 7 matrices (3D Poisson) of different sizes.

avoid doing adding duplicate at this stage. After the first recursive function is finished, we will perform a sorting and then add the duplicates only once at the end.

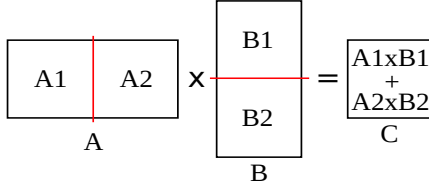


Figure 4: Case 2: When A is horizontal, split A by column and B by row. Call the recursive function twice.

Algorithm 2 Case 2: $C = \text{RECURS_MATMULT2}(A, B)$

Input: A, B

Output: C

- 1: $(A1, A2) = \text{SPLIT_BY_COL}(A)$
 - 2: $(B1, B2) = \text{SPLIT_BY_ROW}(B)$
 - 3: $C \leftarrow \text{RECURS_MATMULT}(A1, B1)$
 - 4: $C \leftarrow \text{RECURS_MATMULT}(A2, B2)$
-

2.1.3 Case 3. When A is vertical, i.e. its row size is greater than its column size, we halve A by row based on its row size and halve B by column (Figure 5). In contrary to the previous case, the column size of B is not related to row size of A, so they are split independently. This time the `RECURS_MATMULT` will be called four times (Algorithm 2). Although we have 4 recursive calls in this case, but there is no duplicates at the end, which makes this case more efficient than Case 2 for the total time, because it is faster to do the sorting and adding duplicates at the end on a smaller set of entries.

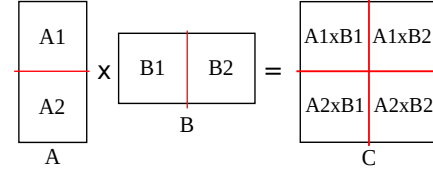


Figure 5: Case 3: When A is vertical, split A by row and B by column. Call the recursive function four times.

Algorithm 3 Case 3: $C = \text{RECURS_MATMULT3}(A, B)$

Input: A, B

Output: C

- 1: $(A1, A2) = \text{SPLIT_BY_ROW}(A)$
 - 2: $(B1, B2) = \text{SPLIT_BY_COL}(B)$
 - 3: $C \leftarrow \text{RECURS_MATMULT}(A1, B1)$
 - 4: $C \leftarrow \text{RECURS_MATMULT}(A2, B1)$
 - 5: $C \leftarrow \text{RECURS_MATMULT}(A1, B2)$
 - 6: $C \leftarrow \text{RECURS_MATMULT}(A2, B2)$
-

We have also implemented splitting based on the number of nonzeros. In Case 2, we split A in a way to have half of nonzeros in A1, and the other half in A2. The same split is used for B. In Case 3, we do the same, but separately for both A and B.

2.1.4 All together. When all three cases work together, we have Case 2 and Case 3, that aim to divide the matrices into skinny matrices such that the resulting matrix is small. Then by using a hybrid multiplication algorithm, we get these results. These results are then accumulated and merged together. From a memory access perspective, the accumulation and merging required for Case 2 and 3 is structured access to the matrix, with the only random access happening during Case 1. This makes the overall algorithm very efficient.

2.2 AMG Matrix-Multiplication: Communication

As noted earlier, to compute the coarse matrix A_c , a triple matrix multiplication is performed:

$$A_c = R \times A \times P \quad (3)$$

with $R = P^T$ in the Galerkin approach, which we use in our implementation. In this section, we explain how the communication is setup to compute the coarse matrix A_c , exploiting properties of the matrix structure specific to AMG. Matrices are partitioned across multiple processors by row blocks (Figure 6). Matrices A and P have the same number of rows and consequently are partitioned the same way. R has fewer number of rows and has a different partition. This is because coarsening need not be uniform across processes. Consequently the partitioning of the rows of R could be different from that of A and P. The triple matrix product is performed in two parts: first $A \times P$ is computed, followed by $R \times B$, where $B = A \times P$ is the result of the first multiplication. In other words, this is equivalent to performing matrix-matrix multiplications (`MATMULT`) twice.

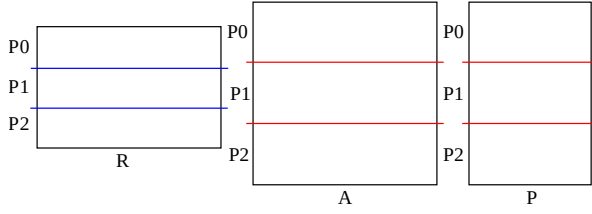


Figure 6: Partitioning of the matrices across the processors in row blocks. A and P have the same partition but R 's is different.

2.2.1 Part 1. In this part, we explain how to compute $B := A \times P$. We assume the same partition of rows of A on also its columns (red lines) since A is square. For columns of P we use the partition of rows of R (blue lines in Figure 7). Without loss of generality, let us focus on how to perform MATMUL on processor $P1$. To compute entry $B(i, j)$, we need to multiply row i of A with column j of P and add them together (since we are working with sparse matrices, we only consider the nonzeros here).

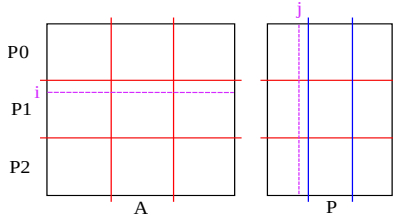


Figure 7: This figure shows how the matrices are split into sub-blocks in Part 1. Column j of P is stored on different processors.

Column j of P is distributed between all the processors. Therefore we need to communicate all nonzeros of that column and then perform $B_{ij} = \sum_k A_{ik} P_{kj}$. Since that can lead to significant communication, we make use of the fact that R is the transpose of P and is already available locally because of the multigrid hierarchy. We note that column blocks of P (e.g. r_0 in Figure 8) are actually row blocks of R transposed (rt_0 , which is transpose of r_0).

We have implemented this part in an overlapped fashion; first we do the send and receive commands (to communicate rt blocks) and while this communication is being done, we perform MATMUL, so saving time for the communication (Algorithm 4). B_i in the algorithm is the row block of matrix B on processor i and B_{ik} is the sub-block result of multiplying A_i with rt_k .

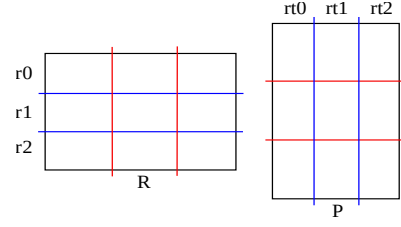


Figure 8: This figure shows how row block of R are transpose of column blocks of P .

Algorithm 4 Part 1: $B_i = A_i \times P$

Input: A_i, R

Output: B_i (result of $A_i \times P$)

- 1: $R1 \leftarrow \text{transpose of } R_i \text{ (locally)}$
 - 2: **for** $k = \text{myrank} : \text{myrank} + \text{nprocs}$ **do**
 - 3: $R2 \leftarrow \text{Irecv}(\text{transpose of } R_{\text{block}}) \text{ from right neighbor}$
 - 4: $\text{Isend}(R1) \text{ to left neighbor}$
 - 5: $B_{ik} \leftarrow \text{RECURS_MATMUL}(A_i, R1)$
 - 6: $\text{wait for Isend and Irecv to finish}$
 - 7: $\text{swap}(R1, R2)$
 - 8: **end for**
 - 9: locally sort B_i and add duplicates
-

2.2.2 Part 2. Now we explain how to do the second MATMUL: $R \times B$. The blocks of R on processor $P1$ in Figure 9, should be multiplied with the corresponding blocks of B with the same color. In contrary to the previous part, we already don't have the transpose of the right-hand side matrix and performing the transpose in parallel is expensive. Instead, we change the way the multiplication is being done and perform a cheaper communication round at the end.

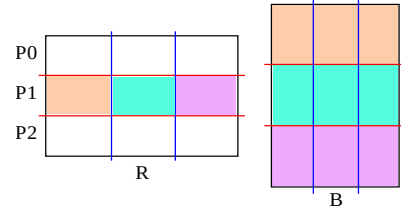


Figure 9: Part 2: $R \times B$. This figure shows which sub-blocks of R should be multiplied by which sub-blocks of B .

In this case we have the transpose of the left-hand side matrix, so we use P instead of R to do this multiplication. We only perform the multiplication of the green blocks on processor $P1$ in Figure 10, which can be done locally. In the previous case each sub-block of the local left-hand side is multiplied by only one sub-block of the local right-hand side. But in this method, each sub-block of local P is being multiplied by the entire row block of B , e.g. P_{10} is multiplied by all B_{10} , B_{11} and B_{12} , and so on.

The difference for final result between this case and the naïve Case 2 is that, the final entries are not on the correct processors, so an additional data exchange needs to be performed at the end

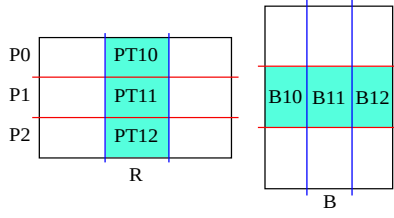


Figure 10: 1

to restore the entries on the correct processes. We sort the entries locally at the end and add the duplicates together. Finally, we sort them globally (using HykSort [15]) and again add the duplicates together (Algorithm 5).

Algorithm 5 Part 2: $Ac = R \times B$

Input: P_i, B_i **Output:** Ac_i

- 1: $PT_i \leftarrow$ transpose of P_i (locally)
 - 2: **for** $k = 0 : nprocs$ **do**
 - 3: $Ac_i \leftarrow \text{RECURS_MATMULT}(PT_{ik}, B_i)$
 - 4: **end for**
 - 5: locally sort Ac_i and add duplicates
 - 6: globally sort Ac_i and add duplicates
-

3 NUMERICAL RESULTS

Our code is written in C++ using MPI and OpenMP and is freely available on github (url withheld for review) under an MIT license. All experiments were conducted on the RMACC Summit Supercomputer at the University of Colorado, Boulder (via XSEDE). Each node has 24 cores and it uses Intel Xeon E5-2680 with 4.84GB of memory per core. All experiments were run in the hybrid MPI+OpenMP mode.

For these experiments for MATMULT we have multiplied a banded matrix with itself, assuming that the matrix is being multiplied with a separate matrix, so not using any information from the left-hand side matrix for the right-hand side one.

Figure11 is the strong scaling for five banded matrices of the same size (192k), but with different bandwidth. The legend shows the density ($\frac{\text{nonzero}}{\text{size}^2}$) of each matrix. Our solver scales consistently for different density values. There is no data in the plot for the matrix with density 0.02 on 24 processors because it was too big to fit in the memory of one node.

Figure12 compares the scaling time for when we split the matrices based on matrix size and when we split based on number of nonzeros. The one that uses the matrix size is more scalable, especially for denser matrices.

Figure13 compares the strong scaling between our solver with PETSc. For the matrices with lower density (more sparse) PETSc performs better when using higher number of processes, but for denser matrices our solver is faster. In multigrid hierarchy, the coarse matrices get denser as we go to lower levels, so it becomes expensive to perform MATMULT at those levels and having an efficient matrix-matrix product will improve the setup cost significantly.

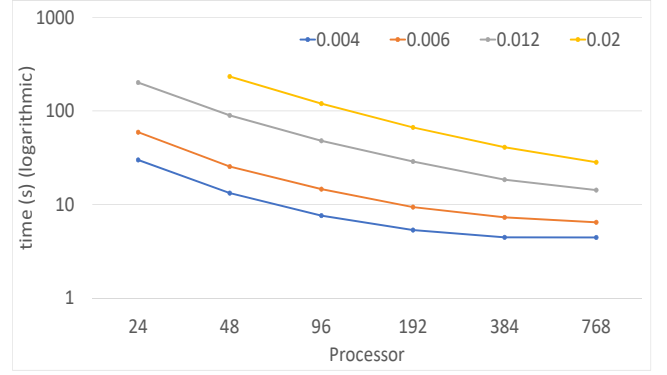


Figure 11: Strong scaling for five banded matrices of the same size (192k), but with different bandwidth. The legend shows the density ($\frac{\text{nonzero}}{\text{size}^2}$) of each matrix.

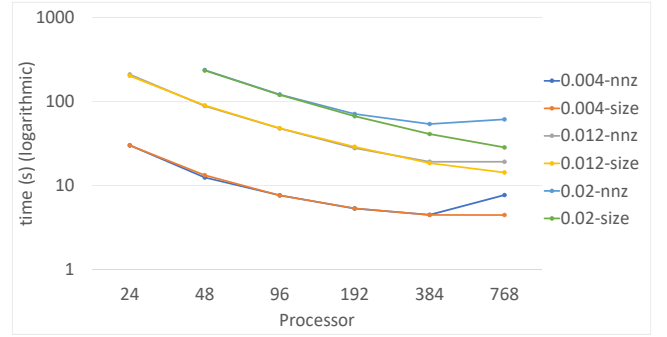


Figure 12: Comparison of the the strong scaling when using two different splitting strategies: based on matrix size and based on number of nonzeros. The legend shows the density of each matrix.

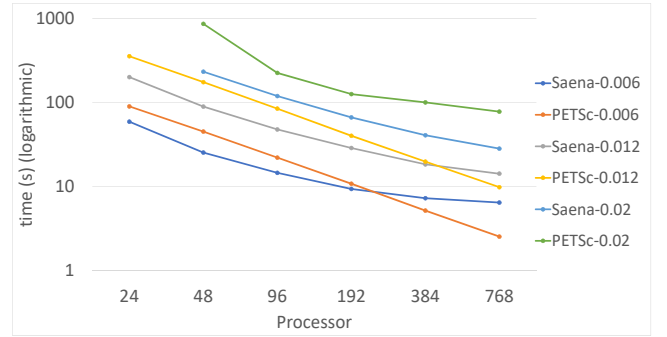


Figure 13: Comparison of the the strong scaling between our solver and PETSc. The number for each line shows the density for that matrix. The legend shows the density of each matrix.

Figure14 shows the weak scaling for two banded matrices: one with 24k on each node and the other one with 100k on each node. Our solver scales better when there is a smaller block of the matrix

on each core, which happens when we use more processors or when the matrix is smaller.

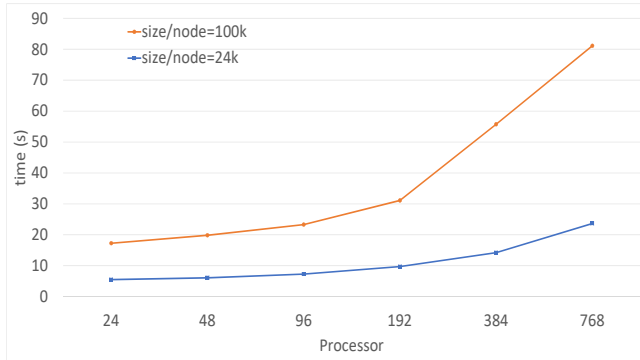


Figure 14: Weak scaling for two banded matrices: blue line shows the one with 24k on each node (1k on each core) and red line shows the larger one with 100k on each node (4166 on each core)

4 CONCLUSION

We have presented a divide and conquer approach to improve the efficiency of matrix-matrix multiplication. We have also designed a low-communication algorithm specific to AMG, to improve the efficiency of the AMG setup phase. We demonstrated performance gains from using our methods and compared our multiplication with the in-built functions within PETSc. In our future work, we want to further improve our performance and scalability and also focus on using sparsification algorithms to ensure the sparsity of coarser levels.

REFERENCES

- [1] N. Bell, S. Dalton, and L. N. Olson. Exposing fine-grained parallelism in algebraic multigrid methods. *SIAM Journal on Scientific Computing*, 34(4):C123–C152, 2012.
- [2] D. Braess. On the combination of the multigrid method and conjugate gradients. In W. Hackbusch and U. Trottenberg, editors, *Multigrid Methods II*, pages 52–64, Berlin, 1986. Springer-Verlag.
- [3] J. H. Bramble and X. Zhang. The analysis of multigrid methods. In *Handbook of numerical analysis, Vol. VII*, Handb. Numer. Anal., VII, pages 173–415. North-Holland, Amsterdam, 2000.
- [4] S. C. Brenner. Smoothers, mesh dependent norms, interpolation and multigrid. *Applied Numerical Mathematics*, 43(1-2):45–56, 2002. 19th Dundee Biennial Conference on Numerical Analysis (2001).
- [5] A. Buluç and J. Gilbert. Parallel sparse matrix-matrix multiplication and indexing: Implementation and experiments. *SIAM Journal on Scientific Computing*, 34(4):C170–C191, 2012.
- [6] J. E. Dendy, Jr. Black box multigrid. *Journal of Computational Physics*, 48(3):366–386, 1982.
- [7] A. Gholami, D. Malhotra, H. Sundar, and G. Biros. Fft, fmm, or multigrid? a comparative study of state-of-the-art poisson solvers for uniform and nonuniform grids in the unit cube. *SIAM Journal on Scientific Computing*, 38(3):C280–C306, 2016.
- [8] F. Gremse, A. Håüfter, L. Schwen, F. Kiessling, and U. Naumann. Gpu-accelerated sparse matrix-matrix multiplication by iterative row merging. *SIAM Journal on Scientific Computing*, 37(1):C54–C71, 2015.
- [9] H. Guillard and P. Vanek. An aggregation multigrid solver for convection-diffusion problems on unstructured meshes. Technical report, 1998.
- [10] Y. Maday and R. Muñoz. Spectral element multigrid. II. Theoretical justification. *Journal of scientific computing*, 3(4):323–353, 1988.
- [11] Y. Notay. Aggregation-based algebraic multilevel preconditioning. *SIAM J. Matrix Analysis Applications*, 27(4):998–1018, 2006.

- [12] Y. Notay. An aggregation-based algebraic multigrid method. *Electronic transactions on numerical analysis*, 37(6):123–146, 2010.
- [13] E. Saule, K. Kaya, and Ü. V. Çatalyürek. Performance evaluation of sparse matrix multiplication kernels on intel xeon phi. In R. Wyrzykowski, J. Dongarra, K. Karczewski, and J. Wańniewski, editors, *Parallel Processing and Applied Mathematics*, pages 559–570, Berlin, Heidelberg, 2014. Springer Berlin Heidelberg.
- [14] H. Sundar, G. Biros, C. Burstedde, J. Rudi, O. Ghattas, and G. Stadler. Parallel geometric-algebraic multigrid on unstructured forests of octrees. In *Proceedings of the International Conference on High Performance Computing, Networking, Storage and Analysis, SC '12*, pages 43:1–43:11, Los Alamitos, CA, USA, 2012. IEEE Computer Society Press.
- [15] H. Sundar, D. Malhotra, and G. Biros. Hyksort: A new variant of hypercube quicksort on distributed memory architectures. In *Proceedings of the 27th International ACM Conference on International Conference on Supercomputing, ICS '13*, pages 293–302, New York, NY, USA, 2013. ACM.
- [16] O. Tatebe and Y. Oyanagi. Efficient implementation of the multigrid preconditioned conjugate gradient method on distributed memory machines. In *Supercomputing'94. Proceedings*, pages 194–203. IEEE, 1994.
- [17] E. Treister and I. Yavneh. Non-galerkin multigrid based on sparsified smoothed aggregation. *SIAM Journal on Scientific Computing*, 37(1):A30–A54, 2015.
- [18] P. Vaněk, M. Brezina, J. Mandel, et al. Convergence of algebraic multigrid based on smoothed aggregation. *Numerische Mathematik*, 88(3):559–579, 2001.
- [19] P. Vanek, J. Mandel, and M. Brezina. Algebraic multigrid by smoothed aggregation for second and fourth order elliptic problems. Technical report, Denver, CO, USA, 1995.
- [20] R. Yuster and U. Zwick. Fast sparse matrix multiplication. *ACM Trans. Algorithms*, 1(1):2–13, July 2005.